Localization and quaternary structure of the PKA RIβ holoenzyme

Ronit Ilouz[a], José Bubis[b], Jian Wu[c], Yun Young Yim[c], Michael S. Deal[c], Alexandr P. Kornev[a,d], Yuliang Ma[a], Donald K. Blumenthal[e], and Susan S. Taylor[a,c,d,1]

[a]Howard Hughes Medical Institute, and Departments of [c]Chemistry and Biochemistry and [d]Pharmacology, University of California at San Diego, La Jolla, CA 92093; [b]Department of Cell Biology, Simon Bolivar University, Caracas 1081-A, Venezuela; and [e]Department of Pharmacology and Toxicology, University of Utah, Salt Lake City, UT 84112

Contributed by Susan S. Taylor, June 6, 2012 (sent for review May 6, 2012)

Specificity for signaling by cAMP-dependent protein kinase (PKA) is achieved by both targeting and isoform diversity. The inactive PKA holoenzyme has two catalytic (C) subunits and a regulatory (R) subunit dimer (R_2:C_2). Although the RIα, RIIα, and RIIβ isoforms are well studied, little is known about RIβ. We show here that RIβ is enriched selectively in mitochondria and hypothesized that its unique biological importance and functional nonredundancy will correlate with its structure. Small-angle X-ray scattering showed that the overall shape of RIβ$_2$:C_2 is different from its closest homolog, RIα$_2$:C_2. The full-length RIβ$_2$:C_2 crystal structure allows us to visualize all the domains of the PKA holoenzyme complex and shows how isoform-specific assembly of holoenzyme complexes can create distinct quaternary structures even though the R_1:C_1 heterodimers are similar in all isoforms. The creation of discrete isoform-specific PKA holoenzyme signaling "foci" paves the way for exploring further biological roles of PKA RIβ and establishes a paradigm for PKA signaling.

structural biology | signal transduction | allostery

Cyclic AMP-dependent protein kinase (PKA) regulates a plethora of biological events that extend from development and differentiation to memory, ion transport, and metabolism. The inactive PKA holoenzyme is composed of a regulatory (R) subunit dimer and two catalytic (C) subunits. Binding of cAMP to the R-subunits unleashes the C-subunits, thereby allowing phosphorylation of PKA substrates. Specificity of PKA signaling is achieved in large part by the isoform diversity of its R-subunits. There are two classes of R-subunits, RI and RII, which are subclassified into α and β subtypes. Each isoform is encoded by a unique gene and is functionally nonredundant. RIα-null mice display early embryonic lethality (1), whereas RIIβ-null mice have a lean phenotype and are resistant to diet-induced diabetes (2). Specific isoforms also are expressed differently in cells and tissues. The RIβ isoform is expressed abundantly in brain and spinal cord (3–5). Hippocampal slices from RIβ-null mice show a severe deficit in long-term potentiation and also in long-term depression and memory. Although RIα protein levels are increased in these mice, the hippocampal function is not rescued, suggesting a unique role for RIβ, which is the least studied R-subunit (6, 7). Most localization studies have focused on the differences between RI and RII and showed that RI isoforms are diffused mainly in the cytoplasm, whereas RIIs typically are associated with membranous organelles. More than 50 A kinase-anchoring proteins (AKAPs) have been identified as targeting PKA to a specific subcellular location (8). The only potential AKAP that binds preferentially to the RIβ isoform identified so far is the neurofibromatosis 2 tumor suppressor protein, merlin (9).

All R isoforms share the same domain organization, which includes a docking and dimerization (D/D) domain followed by an inhibitor sequence and two cAMP-binding domains (Fig. 1*E*). Even though the overall fold of each cAMP-binding domain is conserved, each isoform has a different sensitivity to cAMP activation (10, 11).

Structures of the C-subunit, deletion mutants of various R-subunits, and truncated holoenzyme complexes corresponding to R_1:C_1 heterodimers have been solved; however, neither RIβ alone nor the full-length R dimer has been studied structurally. Although structures of R:C complexes revealed that the R-subunit undergoes major conformational changes upon binding to the C-subunit (12–14), all R:C heterodimer structures identified so far are similar and, therefore, do not explain fundamental isoform differences. These R:C complexes, which lack the D/D domain, cannot explain how the holoenzymes are targeted to specific sites by docking to AKAPs, and they do not tell us whether there are interactions between the two R:C heterodimers. Small-angle X-ray/neutron scattering (SAXS/SANS) showed profound differences in the overall shape of the full-length RIα, RIIα, and RIIβ holoenzymes (15, 16). A recently described structure of a deletion mutant of RIα (75–244):C containing an extended linker shows how the linker interacts with the symmetry-related dimer (17) and thereby creates a twofold axis of symmetry between the two heterodimers. This structure provides a plausible model explaining how a dimer of heterodimers can be assembled. Most recently, the structure described for the RIIβ holoenzyme shows that its quaternary structure differs dramatically from the model of the RIα holoenzyme (18) and shows how differently the C-subunit can be packaged by two functionally nonredundant R-subunits. However, none of the D/D domains of the R-dimer in the holoenzyme complex have been visualized, and the full allosteric potential that is embedded in each holoenzyme structure remains elusive.

Results

PKA RIβ Subunit Is Enriched in Mitochondrial Fractions. Although RIα and RIβ isoforms have similar domain organization and share 87% sequence identity (Fig. S1), they are not functionally redundant functionally. So far there has been no systematic comparison of the cell distribution of RIα vs. RIβ. Because differences in function often are associated with subcellular localization and targeting, we first examined the localization pattern of all R isoforms in mouse heart using sorbitol gradient centrifugation, by which RIα and RIβ can be distinguished based on differences in gel mobility. Interestingly, we found that RIβ is the only isoform that is enriched selectively in the heavy membrane fractions that correspond to mitochondria and comigrated primarily with the mitochondrial marker cytochrome C (Fig. 1*A*). In contrast, RIα, which typically is cytoplasmic (22), is seen in the soluble fractions and the Golgi. RII isoforms are distributed

Author contributions: R.I., J.B., A.P.K., and S.S.T. designed research; R.I., J.B., J.W., Y.Y.Y., M.S.D., Y.M., and D.K.B. performed research; J.B. and M.S.D. contributed new reagents/analytic tools; R.I., J.W., A.P.K., and S.S.T. analyzed data; and R.I., A.P.K., D.K.B., and S.S.T. wrote the paper.

The authors declare no conflict of interest.

Freely available online through the PNAS open access option.

Data deposition: The atomic coordinates and structure factors have been deposited in Protein Data Bank, www.pdb.org (PDB ID code 4DIN).

[1]To whom correspondence should be addressed. E-mail: staylor@ucsd.edu.

This article contains supporting information online at www.pnas.org/lookup/suppl/doi:10.1073/pnas.1209538109/-/DCSupplemental.

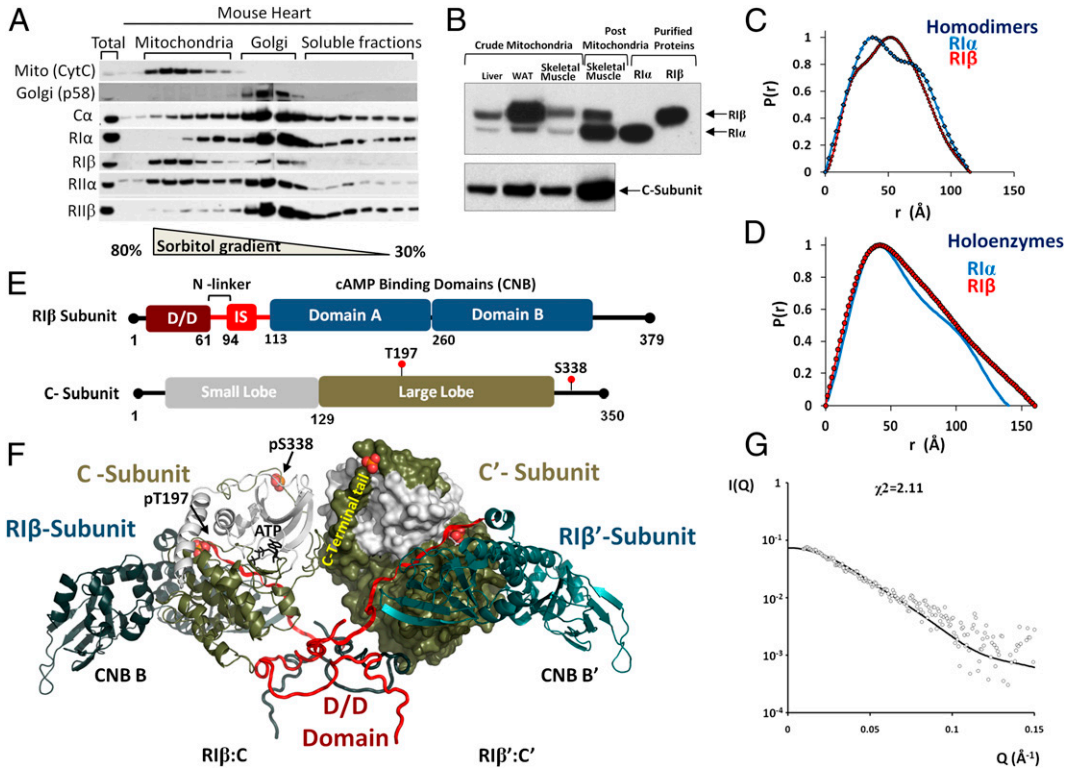

Fig. 1. RIα and RIβ holoenzymes have different subcellular distributions and unique architectures. (*A*) Postnucleus homogenates of mouse heart tissues were separated by sorbitol gradient. Cytochrome C was used as a marker for mitochondria and p58 as a marker for Golgi. Equal volumes of each fraction were analyzed with specific antibodies for each isoform. Total cell lysate is shown in the first lane. (*B*) RIα and RIβ expression was detected in enriched mitochondrial fractions from mouse liver, white adipose tissues, and skeletal muscle using RIα antibody that recognizes both RI isoforms at the same intensity. Post-mitochondria fractions from skeletal muscle depleted of mitochondria as well as RIα and RIβ purified proteins were used as controls. (*C*) P(r) functions as calculated from SAXS data for RIβ and RIα homodimers. (*D*) P(r) functions as calculated from SAXS data for $RI\beta_2{:}C_2$ and $RI\alpha_2{:}C_2$ holoenzymes. (*E*) Domain organization of R- and C-subunits. (*F*) Crystal structure of the full-length $RI\beta_2{:}C_2$ quaternary complex. The holoenzyme is labeled RIβ:C and the second holoenzyme, generated by the crystallographic twofold symmetry, is labeled RIβ′:C′. N-lobes of the C-subunits are colored white, C-lobes are colored tan. R-subunits are colored teal. The N-terminal parts of R-subunits are colored red and blue. Phosphorylation sites are orange/red spheres. ATP is black. (*G*) Fit of the simulated scattering curve to the experimental data. The SAXS curve was computed from the RIβ tetrameric holoenzyme shown in *D*. Dots represent experimental data for RIβ tetrameric holoenzyme.

throughout. We further confirmed the mitochondrial localization of RIβ by isolating mitochondria from different mouse tissues. As seen in Fig. 1*B*, RIβ, as compared with RIα, is enriched in mitochondria from all the tissues tested, with especially high levels in perirenal white adipose tissue. As expected, RIα is predominant in the residual postmitochondrial fraction from skeletal muscle (Fig. 1*B*). RIα was shown previously to be targeted only in response to certain stimuli such as capping with an antigen (19) or generation of reactive oxygen species (20). The selective targeting of RIβ seen only when one enriches for mitochondria suggests that RIβ may have a unique role in regulating mitochondrial structure and/or function.

Based on SAXS, RIα and RIβ Holoenzymes Have Unique Architectures. We hypothesized that the unique biological importance of RIα and RIβ and the differences in their tissue distribution also might be reflected in isoform-specific architectures. After purifying the full-length RIβ and forming the RIβ holoenzyme, we first confirmed that the RIβ holoenzyme has a lower K_a (cAMP) for activation than the RIα holoenzyme, 29 nM vs. 103 nM, respectively, as previously described (10). To compare their structures, we first used SAXS. The full-length RIβ and RIα homodimers have the same maximum dimension, D*max* (115 Å) and radius of gyration (R*g*) values (40 Å) and thus exhibit a similar solution structure which is markedly more compact than the extended RII-type homodimer structures (Fig. 1*C*) (16). However, significant differences are seen in the overall shape of the corresponding full-length RIβ and RIα holoenzymes (Fig. 1*D*). The RIβ holoenzyme has a linear slope in the high distance (*r*) range with an Rg of 52Å and a D*max* of around 165 Å, suggesting an extended cylinder-like shape (Fig. 1*D* and Fig. S2*A*). In contrast, previous SAXS and SANS analysis showed that the RIα tetrameric holoenzyme is more compact and V-shaped, with an Rg of 47Å and a D*max* of 140Å (15, 16). The P(r) curve of the RIα holoenzyme with its characteristic broad shoulder in the high *r* region is shown in Fig. 1*D*. These two RI holoenzyme shapes also are quite different from the compact globular shape of the RIIβ holoenzyme and the extended RIIα dumbbell-shaped holoenzyme (16). Taken together, the SAXS data demonstrate that, in the absence of the C-subunit, RIα and RIβ homodimers have similar overall compact shapes, but significant differences in their shapes emerge when these isoforms are assembled into a dimer of heterodimers. Moreover, based on SAXS, the quaternary shapes of all four PKA holoenzymes are different.

Given the differences in subcellular distribution and sensitivity to activation by cAMP, as well as the unique overall architectures of RIα and RIβ, we hypothesized that the assembly of the R:C subunits in their holoenzyme conformation will each have unique quaternary structures for each isoform.

Crystal Structure of the RIβ Quaternary Holoenzyme Complex. By crystallizing the wild-type full-length RIβ dimer bound to two full-length C-subunits including ATP and two Mg^{+2} ions, we obtained a PKA holoenzyme structure at 3.7-Å resolution (Fig. 1*F*, Fig. S2*B*, and Table S1). The C-subunit adopts a closed conformation with Mg_2ATP and the inhibitor site of the R-

subunit bound at the active site cleft, similar to previous RIα holoenzyme structures (21, 22). The R:C binding interface of each heterodimer in the RIβ structure also is similar to previous heterodimer structures: RIα (91–379):C, RIIα(91–392):C, and RIIβ (103–268):C (12–14). The interface lies primarily between the C-subunit and cAMP-binding domain A (CNB-A) of the R-subunit, whereas cAMP-binding domain B extends the interaction surface and contacts the αH–αI loop in the C-subunit.

The unique isoform-specific conformation of the RIβ holoenzyme can be appreciated only in the full-length holoenzyme, which is a dimer of two heterodimers (marked as R:C and R′:C′ in the figures). As in the RIα and RIIβ holoenzymes, the two heterodimers come together to create a twofold axis of symmetry; however, the details of that interface are different in each holoenzyme. These interfaces are created by loops and linkers that are exposed to solvent in the heterodimers.

The major interface between the two heterodimers in the RIβ tetramer involves the C-terminal tails of both C-subunits (406 Å^2) (Fig. 2 and Fig. S3). The C-terminal tail of the C-subunit (residues 301–350) is a conserved structural element of most AGC kinases, and the unique features in the core of most AGC kinases are conserved to integrate the core functionally with the C-terminal tail to create an active enzyme (23, 24). The C-terminal tail can be divided into three segments. The C-lobe tether (CLT) is tightly anchored to the large C-terminal lobe, and the N-lobe tether (NLT) is anchored firmly to the small N-terminal lobe. These two segments lock the C-subunit into its active conformation. The active site tether (AST) that links these two segments is dynamic and locks the kinase into a closed conformation in the presence of nucleotides (Fig. S3) (23, 25, 26). The FDDY motif (residues 327–330) is the signature motif of the AST and interacts directly with ATP. F327 is the only residue outside the kinase core that binds to the adenine ring. Y330 lies on top of the ribose (Fig. S3). Both F327 and Y330 are essential for activity (26, 27).

The RIβ holoenzyme structure contains ATP, and we can see clearly that the AST is anchored to the active site, as it is in all nucleotide-bound structures of the C-subunit and in the RIα holoenzymes (21, 22). The interface between the two heterodimers is created by the antiparallel alignment of the two C-tails, specifically between S325 from one C-tail and D329 from the FDDY motif from the symmetry-related C-tail (Fig. 2*B*). The FDDY motif in the C-terminal tail thus is bifunctional. It acts not only as a *cis*-regulatory element that is needed for the catalytic activity and recruitment of ATP but also can be a *trans*-regulatory element that mediates interactions between the two C-subunits in the RIβ holoenzyme. In the RIβ holoenzyme the FDDY motif carries out both functions.

The C-tail is multifunctional and highly regulated in every AGC kinase. The FDDY motif in the C-terminal tail of some AGC kinases (e.g., Akt, PRK2, and PKA) is thought to serve as an important docking site for PDK1, which lacks its own FDDY motif (28); the recently explained structure of full-length PKCβII shows how the Phe residue of the FDDY motif also can serve as a docking site for its own C1B domain (29). There also is a critical phosphorylation site in the C-tail that, in the case of PKA, is added cotranslationally while the C-subunit is still on the ribosome. In PKC this phosphorylation site is a docking site for Pin1 (30). Most other AGC kinases have an additional phosphorylation site that lies just beyond the hydrophobic (HF) motif. A conserved PXXP motif in Akt can interact with Src or, in the case of PKCβII, with Hsp70/cdc43 (31). Thus many protein:protein interaction motifs are embedded within the C-tail, and these interactions define the C-tail as a dynamic *trans*-regulatory element. The RIβ structure provides additional insights into the versatility and functional importance of these motifs embedded within the C-terminal tail of the AGC kinases.

D/D Domain Allows the Complex to Sense AKAP Binding Globally. The unusual feature of our structure was that we were capable to visualize both the D/D domain and the CNB domains

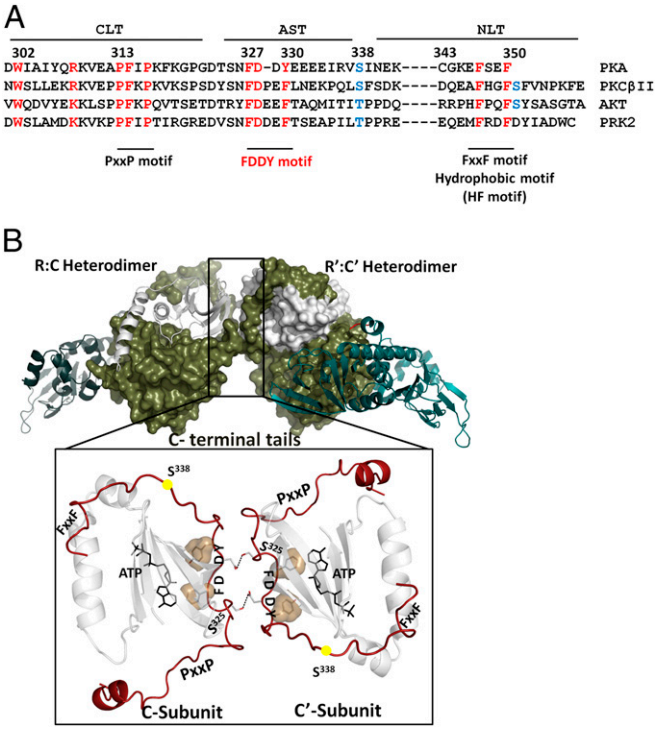

Fig. 2. The C-terminal tail of the C-subunit is a docking interface between the two heterodimers. (*A*) Alignment of four AGC kinases. The three major segments, NLT, CLT, and AST are marked. (*B*) The interface between the two heterodimers. In the close-up view the C-terminal tails are shown in red. Specific interactions that involve the FDDY motif are shown. ATP is shown in black.

simultaneously. Structures of these domains for different R-subunits were solved previously only separately. The extended flexible linker between these domains prevented crystallization of the full length R-subunits. Because the heterodimer structures lack the D/D domain, they do not provide a detailed picture of the molecular interactions of the full-length holoenzyme and potential interactions between the D/D domain and the rest of the complex, nor do they explain fully the mechanism for allostery and regulation. Fig. 3 and Fig. S4 highlight the position of the full-length R-subunit homodimer containing the D/D domain as well as the CNB domains. Although 21 residues of the linker region between the D/D domain and the CNB-A domain of each R-subunit (residues 59–81) are still missing in our structure, several features are clear. The CNB domains in each protomer are well separated, in contrast to our RIα model and the RIIβ holoenzymes, in which the CNB domains are a major interface. In all cases the CNB domains undergo a major conformational change upon release of cAMP and binding to the C-subunit. However, the C-subunit–bound conformation of all R-subunits is virtually the same (Fig. S5). Thus, it is the unique interface created by each R:C heterodimer that defines the particular quaternary structures of each holoenzyme.

In the RIβ holoenzyme the D/D domain is an integral part of the holoenzyme complex, providing direct communication between the heterodimers; it not only dimerizes the two R-subunits and provides the docking surface for the AKAP helix (32–34) but also docks onto a well-known hydrophobic binding site in the adjacent symmetry-related C-subunit (Fig. S4*A* and Figs. S6*A* and S7).

A specific feature of the RI subunits is the N-terminal helix (named "helix N") and the presence of cysteine residues (Fig. S4*C*). In the isolated RIα D/D domain structures, Cys37 from one chain is disulfide bonded to Cys16 from the opposite protomer (32, 34). This disulfide bond also is present in the isolated

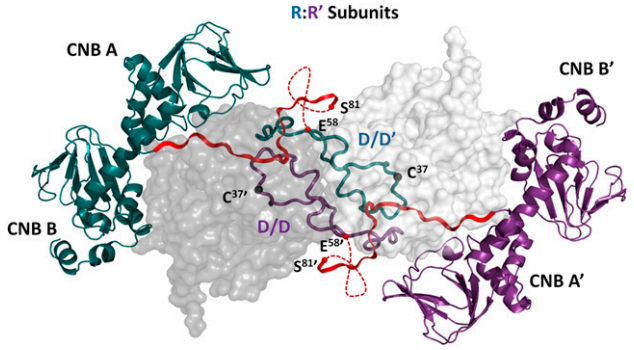

Fig. 3. Overview of the full-length RIβ dimer in the holoenzyme structure. Overall structure of the RIβ dimer. The monomers, marked as R and R′, are shown in teal and purple. The linker region is shown in red. Residues missing in the density map are denoted by dashed lines.

RIα D/D domain bound to an AKAP peptide (Fig. S4*B*) (34). In the RIβ holoenzyme complex, the D/D domain is an integral part of the intact holoenzyme, and Cys37 is not disulfide bonded; instead, it is bound to the C-subunit (Figs. 3 and 4*A*). This bond allows helix N to be more flexible, similar to the isolated RIα D/D domain in reduced conditions in which these cysteines are not disulfide bonded. Based on NMR studies, the linker between helix N and helix I is dynamic (32). In the isolated RIα D/D domain structure, residues 24–38 are defined as helix I flanked by linker regions. In the RIβ tetramer, however, the D/D domain helices are not well formed. In particular, residues 35–38 are not part of helix I when they dock onto the C-subunit (Fig. S4*A*). This observation may suggest flexibility or plasticity of the D/D domain when it mediates interdomain interactions. Because introducing the disulfide bonds obviously alters this region, we can begin to appreciate how this domain might allow the RI subunits to function as unique redox sensors (20, 35). Recently, it was shown in cardiac myocytes that, upon H_2O_2 treatment, there is increased disulfide-bond formation in the RIα D/D and nuclear localization of PKA, an effect attributed to the enhanced anchoring by AKAPs (20). With this structure we see that change of the redox potential could simply lead to reorganization of an AKAP-anchored holoenzyme. We predict that binding of an AKAP, as well as oxidation of disulfide bonds, will have a major effect on the function and dynamic properties of the RIβ holoenzyme.

D/D Domain Interacts with the C-Lobe of the C-Subunit. A second interface for intermolecular interactions between heterodimers in the RIβ holoenzyme is created by the D/D domain of the R-subunit docking onto a hydrophobic pocket in the large lobe of the C′-subunit of the adjacent heterodimer (302 Å^2). Specifically, residues 35–41, localized in the loop that lies between the two helices in the D/D domain, dock onto a conserved substrate binding groove that is formed by residues Tyr235 and Phe239 of the αF–αG loop (Fig. 4*A* and Fig. S6*A*). This hydrophobic interface is formed by two additional residues from the C-subunit: Ala233 and the conserved Pro258 that follows the αG helix. This conserved hydrophobic site is anchored firmly to the central αF-helix that serves as a general scaffold for most of the important residues in all protein kinases (36).

The main chain conformation of the αF–αG loop in the C-subunit is conserved throughout the protein kinase family and is as an important docking site on PKA and other kinases. This hydrophobic pocket created by Tyr235 and Phe239 is recognized in unique ways by different PKA substrates and inhibitors (Fig. S7). For example, an amphipathic helix in the heat-stable protein kinase inhibitor peptide docks onto this pocket (37). The RIIβ subunit occupies the same pocket with a strand region that lies N-terminal to the inhibitor site (N-linker) when the C-subunit is trapped as a ternary complex with nonhydrolyzable analog of ATP, Adenylyl-imidodiphosphate (AMP-PMP) (Fig. S7*C*) (12). In contrast to RIβ, in the holoenzyme model of RIα this pocket interacts with the β4–β5 loop of the R-subunit from the symmetry-related dimer, providing a completely different intermolecular docking surface (Fig. S7*D*) (17). In summary, a portion of the D/D domain docks in a *trans* manner onto a conserved docking site on the C-subunit and appears to be an integral part of the quaternary structure. Although the D/D domain is the least resolved region of the structure, its strategic position suggests that binding to an AKAP will be sensed by the entire holoenzyme.

Flexible Linkers and Loops Direct Holoenzyme Assembly. The greatest sequence variability in the R-isoforms is seen in the linker region between the D/D domain and the cAMP-binding domains. The entire linker segment that joins the D/D domain to CNB-A is classified as an intrinsic disordered region, and embedded within

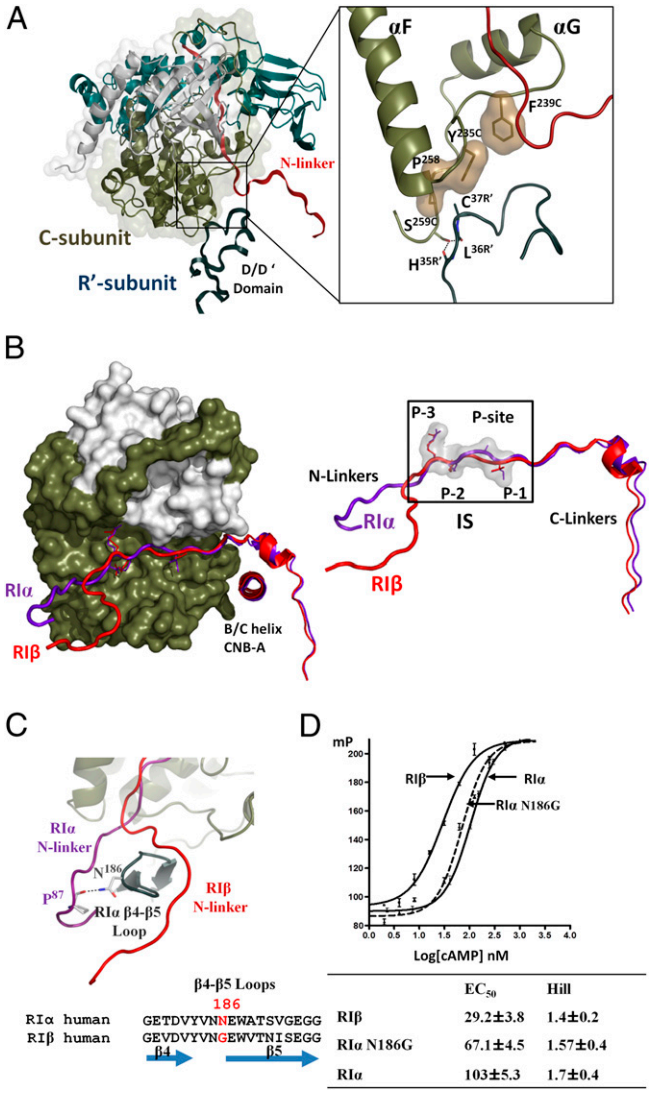

Fig. 4. Variation in the position of the region that lies N-terminal to the inhibitor site. (*A*) The D/D domain (teal) from the R′:C′ heterodimer docks onto the C-subunit (tan) of the adjacent R:C heterodimer. Specific interactions are shown in the close-up view. (*B*) (*Left*) Superposition of RIβ (red) and RIα (purple) inhibitor sequences including N- and C- linkers. (*Right*) Detailed structural comparison. (*C*) A close-up view of the β4–β5 loop (gray) of RIα and the N-linkers of RIα (magenta) and RIβ (red) in the quaternary structures. Sequence alignment of the β4–β5 loops of RIα and RIβ are shown. (*D*) cAMP-induced activation of PKA for the wild-type RIα, RIβ, and RIα N186G mutant, monitored by FAP-IP20 binding.

this segment is the inhibitor site (IS) that docks to the active site cleft of the C-subunit in the holoenzyme. The region from the IS to CNB-A becomes ordered in the holoenzyme (Fig. 4*B*). Superposition of the available structures of the N-linkers of RIα and RIβ shows how each N-linker region docks onto the surface of the C-subunit in a different way, although the structure and position of the inhibitor site and the C-linker of these isoforms, including RIIα and RIIβ, are similar (Fig. 4 *B* and *C*). The structure of the $RIα_1$:C_1 heterodimer that includes its N-linker region shows the importance of this linker for the assembly of the quaternary structure (17). This N-linker docks onto the R-subunit of the symmetry-related dimer and thus creates an interface that enables us to build an RIα holoenzyme model that is a dimer of a heterodimer (17). All R isoforms dock in a similar manner to the active site cleft of the C-subunit, and the overall architecture of the R_1:C_1 heterodimers is remarkably similar (Fig. S8) (12–14). This variability in the R-subunit linker region is used to promote different interdomain arrangements that lead to remarkably different quaternary architectures (Fig. 5). It emphasizes the importance of short linker regions within multidomain proteins: They allow independent functions for each domain and allow structural flexibility, and they also contribute to the unique overall architecture of the protein.

The holoenzyme R_2:C_2 structures show how PKA uses similar building blocks to create unique quaternary structures for each isoform despite the high degree of sequence identity (Fig. 5). In comparing the sequences of RIα and RIβ (Fig. S1), one sees very few changes, especially if one looks only from the inhibitor sites through the C terminus, and most of the differences are conservative. One exception, however, that is significantly different and strategically placed is residue 186 in the β4–β5 loop. This highly conserved loop is solvent exposed in all our previously solved R-subunit structures. In our model of the RIα holoenzyme, however, and in a recently solved structure of the RIIβ quaternary complex, we discovered a function for this motif. Asn186, which is uniquely conserved in RIα but is replaced by Gly in RIβ (Fig. 4*C*), makes a specific contact with the N-linker region of the other heterodimer and thus appears to drive the assembly of the two heterodimers into a tetramer. To test whether a single strategically placed residue can drive the organization of the isoform-specific quaternary structures, we replaced Asn186 with Gly in RIα. As seen in Fig. 4*D* and Fig. S9, this single amino acid replacement results in significant changes in RIα function and structure and causes it to resemble RIβ more closely. The K_a of activation was reduced to 67 nM, a value that lies between the wild-type RIα (103 nM) and the RIβ (29 nM) holoenzymes. The Hill coefficient value of the mutant (1.57), when compared with the wild-type RIα (1.7) and RIβ holoenzymes (1.4), suggests that this single mutant is more RIβ-like (Fig. 4*D*). In addition, its SAXS profile indicates a global conformation different from that seen with the wild-type RIα, and with the R*g* value reduced by 6 Å, a significant change (Fig. S9). Thus the distinct allosteric networks for each isoform and their functional diversity can be achieved by creating specific interfaces in each quaternary structure.

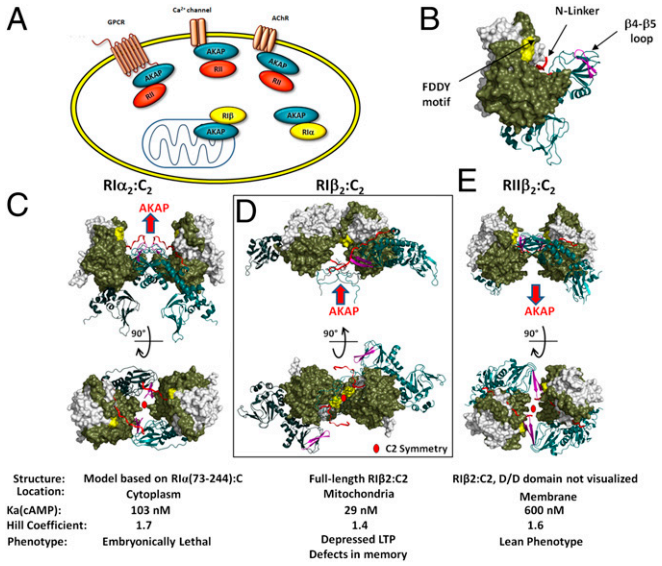

Fig. 5. Specific motifs define isoform-specific interfaces between heterodimers. (*A*) PKA is anchored to scaffolds that assemble macromolecular complexes and define foci for PKA signaling. The complexity of PKA signaling now needs to be considered in light of the targeted holoenzymes that create unique foci for PKA signaling in every cell. These foci will depend on which PKA isoforms and AKAPs are expressed in any given cells as well as on the targeted PKA substrates. RIα typically is cytoplasmatic, RIβ is enriched in the mitochondria, and RIIs are localized to membranes. (*B*) Two motifs that play important roles in the assembly of each tetramer and the N-linker (red) of RIβ holoenzyme are highlighted. The β4–β5 loop is purple, and the FDDY motif is yellow. (*C*–*E*). The quaternary structures of RIα, RIβ, and RIIβ, shown on the top, highlight the differences in the overall architecture of each complex and also indicate the differences in the positioning of the D/D domain (red arrows) and AKAP binding. The twofold axis of symmetry (●) is indicated. The 90° rotation allows one to appreciate the twofold symmetry that is found in each quaternary structure as well as how the two motifs, the β4–β5 loops and the FDDY motifs, contribute to the assembly of the holoenzyme complex. (*C*) A model of the $RIα_2$:C_2 tetrameric holoenzyme based on the RIα(73–244):C structure (17). (*D*) Full-length $RIβ_2$:C_2 crystal structure. (*E*) $RIIβ_2$:C_2 structure. The D/D domain was not visualized, but its position is proposed (18).

Discussion

The RIβ quaternary structure reveals how the PKA holoenzyme uses the R- and C-subunits as dynamic building blocks with the C-subunit serving as a stable scaffold that is embedded in unique ways within the flexible domains of the R-subunit homodimer. Each R_1:C_1 heterodimer is similar in all isoforms, but the two heterodimers interact in unique ways. By forming dimer of dimers in the holoenzyme, we see a twofold symmetrical complex. However, the geometry of the symmetry is unique for each holoenzyme (Fig. 5). In the recently solved structure of the RIIβ holoenzyme (18), as well as in the model of the RIα holoenzyme, the two C-subunits do not touch one another, in contrast to the RIβ holoenzyme (Fig. 5), and the interfaces between the two heterodimers in each isoform are completely different. Each holoenzyme senses cAMP differently, with K_as varying from 30 nM for RIβ to 600 nM for RIIβ; based on our structures of the full-length proteins, it is clear that the allosteric mechanism is isoform specific. Elucidating the details of this mechanism is our next challenge.

The D/D domain, in theory, can function either as an independent docking motif, as was predicted for RIIα (16), or, alternatively, can be an integral part of the holoenzyme that influences the kinase and/or CNB domains. In the RIβ holoenzyme structure we see that the D/D domain interacts directly with the C-subunit. This interaction emphasizes an important role for the D/D domain in assembling the quaternary structure in various PKA isoforms. It also confirms the plasticity and versatility of this domain that allows specific interactions with numerous AKAPs (38). In particular, striking differences are seen in the position of the D/D domain relative to the rest of the protein in the RIβ and RIα holoenzymes (Fig. 5). In addition to being an integral part of the complex, the unique D/D domain position may contribute to its localization and specific AKAP binding in RIβ.

Unlike many protein kinases, PKA is assembled as a fully phosphorylated enzyme that then is packaged as an inactive tetrameric holoenzyme. This fully phosphorylated native state of PKA ensures that PKA activation depends exclusively on the generation of the second messenger, cAMP. Specificity is achieved not only by the tissue-specific expression of the different isoforms but also by targeting the holoenzymes in close proximity to dedicated substrates, typically through AKAP scaffolds. In this way the cell creates microenvironments of PKA signaling that

frequently also include phosphatases and phosphodiesterases. Thus, in cells PKA is packaged as an inactive quaternary structure that is part of a macromolecular complex dedicated to a specific phosphorylation event or a set of correlated events. Most AKAPs that target PKA to channels, transporters, and G protein-coupled receptors are specific for RII subunits, and RII holoenzymes, in general, are constitutively targeted with high affinity to membranes (Fig. 5*A*). In contrast, RIα is thought usually to be cytoplasmic and targeted in response to cell stimuli. Several dual-specific AKAPs bind with high affinity to both RI and RII subunits (39), and a few, such as SKIP and Rapsyn, are specific for RI (40, 41). SKIP specifically localizes RI to the mitochondrial intermembrane space. Here we show that RIβ, not RIα, is selectively enriched in mitochondria. Obviously, now it is essential to elucidate the biological consequences of targeting RIβ to mitochondria.

Conclusion

We now are confronted with the realization that the four PKA holoenzymes not only are functionally nonredundant and localized differently but are also structurally distinct. These results also clearly define PKA not as a single catalytic subunit that floats freely around the cell but as a major regulatory component of complex and highly dynamic macromolecular scaffolds. Each scaffold is dedicated to the regulation of a specific biological event, such as opening and closing a channel or fission vs. fusion of mitochondria. Clearly there also is a mechanism for targeting PKA to the nucleus, where it can mediate gene expression. However, each of these events is likely to be highly orchestrated and almost certainly will be isoform-specific. We know little about the biological role of RIβ, but its structure and its selective enrichment in mitochondria, like the earlier genetic studies, suggest not only that it will be different from the RII-subunits but also that it will be distinct from RIα.

Material and Methods

Details of protein expression holoenzyme formation, crystallization, and refinement, SAXS, and detection of PKA expression in mice are provided in *SI Materials and Methods*. The atomic coordinates have been deposited in the Protein Data Bank (PDB ID 4DIN). All structural figures were prepared using PyMol (http://www.pymol.org).

ACKNOWLEDGMENTS. We thank Corie Y. Ralston and Banumathi Sankaran from the Advanced Light Source beamline 8.2.2 for their assistance; Lynn Ten Eyck and Ganapathy N. Sarma for valuable discussions; and members of the S.S.T. laboratory for helpful discussions about the manuscript. We thank Dr. Jill Trewhella for the use of laboratory facilities at the University of Utah. X-ray scattering data were collected at the University of Utah using facilities supported by the U.S. Department of Energy Grant No. DE-FG02-05ER64026 (to Jill Trewhella). This work was supported by National Institutes of Health Grants DK54441 and GM34921 (to S.S.T.).

1. Amieux PS, et al. (1997) Compensatory regulation of RIalpha protein levels in protein kinase A mutant mice. *J Biol Chem* 272:3993–3998.
2. McKnight GS, et al. (1988) Analysis of the cAMP-dependent protein kinase system using molecular genetic approaches. *Recent Prog Horm Res* 44:307–335.
3. Clegg CH, Cadd GG, McKnight GS (1988) Genetic characterization of a brain-specific form of the type I regulatory subunit of cAMP-dependent protein kinase. *Proc Natl Acad Sci USA* 85:3703–3707.
4. Solberg R, Taskén K, Keiserud A, Jahnsen T (1991) Molecular cloning, cDNA structure and tissue-specific expression of the human regulatory subunit RI beta of cAMP-dependent protein kinases. *Biochem Biophys Res Commun* 176:166–172.
5. Cadd G, McKnight GS (1989) Distinct patterns of cAMP-dependent protein kinase gene expression in mouse brain. *Neuron* 3:71–79.
6. Brandon EP, et al. (1995) Hippocampal long-term depression and depotentiation are defective in mice carrying a targeted disruption of the gene encoding the RI beta subunit of cAMP-dependent protein kinase. *Proc Natl Acad Sci USA* 92:8851–8855.
7. Huang YY, et al. (1995) A genetic test of the effects of mutations in PKA on mossy fiber LTP and its relation to spatial and contextual learning. *Cell* 83:1211–1222.
8. Wong W, Scott JD (2004) AKAP signalling complexes: Focal points in space and time. *Nat Rev Mol Cell Biol* 5:959–970.
9. Grönholm M, et al. (2003) Merlin links to the cAMP neuronal signaling pathway by anchoring the RIbeta subunit of protein kinase A. *J Biol Chem* 278:41167–41172.
10. Cadd GG, Uhler MD, McKnight GS (1990) Holoenzymes of cAMP-dependent protein kinase containing the neural form of type I regulatory subunit have an increased sensitivity to cyclic nucleotides. *J Biol Chem* 265:19502–19506.
11. Zawadzki KM, Taylor SS (2004) cAMP-dependent protein kinase regulatory subunit type IIbeta: Active site mutations define an isoform-specific network for allosteric signaling by cAMP. *J Biol Chem* 279:7029–7036.
12. Brown SH, Wu J, Kim C, Alberto K, Taylor SS (2009) Novel isoform-specific interfaces revealed by PKA RIIbeta holoenzyme structures. *J Mol Biol* 393:1070–1082.
13. Kim C, Cheng CY, Saldanha SA, Taylor SS (2007) PKA-I holoenzyme structure reveals a mechanism for cAMP-dependent activation. *Cell* 130:1032–1043.
14. Wu J, Brown SH, von Daake S, Taylor SS (2007) PKA type IIalpha holoenzyme reveals a combinatorial strategy for isoform diversity. *Science* 318:274–279.
15. Heller WT, et al. (2004) C subunits binding to the protein kinase A RI alpha dimer induce a large conformational change. *J Biol Chem* 279:19084–19090.
16. Vigil D, Blumenthal DK, Taylor SS, Trewhella J (2006) Solution scattering reveals large differences in the global structures of type II protein kinase A isoforms. *J Mol Biol* 357: 880–889.
17. Boettcher AJ, et al. (2011) Realizing the allosteric potential of the tetrameric protein kinase A RIα holoenzyme. *Structure* 19:265–276.
18. Zhang P, et al. (2012) Structure and allostery of the PKA RIIβ tetrameric holoenzyme. *Science* 335:712–716.
19. Skålhegg BS, et al. (1994) Location of cAMP-dependent protein kinase type I with the TCR-CD3 complex. *Science* 263:84–87.
20. Brennan JP, et al. (2006) Oxidant-induced activation of type I protein kinase A is mediated by RI subunit interprotein disulfide bond formation. *J Biol Chem* 281: 21827–21836.
21. Kim C, Xuong NH, Taylor SS (2005) Crystal structure of a complex between the catalytic and regulatory (RIalpha) subunits of PKA. *Science* 307:690–696.
22. Zheng J, et al. (1993) 2.2 A refined crystal structure of the catalytic subunit of cAMP-dependent protein kinase complexed with MnATP and a peptide inhibitor. *Acta Crystallogr D Biol Crystallogr* 49:362–365.
23. Batkin M, Schvartz I, Shaltiel S (2000) Snapping of the carboxyl terminal tail of the catalytic subunit of PKA onto its core: Characterization of the sites by mutagenesis. *Biochemistry* 39:5366–5373.
24. Kannan N, Taylor SS, Zhai Y, Venter JC, Manning G (2007) Structural and functional diversity of the microbial kinome. *PLoS Biol* 5:e17.
25. Kannan N, Haste N, Taylor SS, Neuwald AF (2007) The hallmark of AGC kinase functional divergence is its C-terminal tail, a cis-acting regulatory module. *Proc Natl Acad Sci USA* 104:1272–1277.
26. Yang J, et al. (2009) Contribution of non-catalytic core residues to activity and regulation in protein kinase A. *J Biol Chem* 284:6241–6248.
27. Kennedy EJ, Yang J, Pillus L, Taylor SS, Ghosh G (2009) Identifying critical non-catalytic residues that modulate protein kinase A activity. *PLoS ONE* 4:e4746.
28. Biondi RM, et al. (2002) High resolution crystal structure of the human PDK1 catalytic domain defines the regulatory phosphopeptide docking site. *EMBO J* 21:4219–4228.
29. Leonard TA, Różycki B, Saidi LF, Hummer G, Hurley JH (2011) Crystal structure and allosteric activation of protein kinase C βII. *Cell* 144:55–66.
30. Abrahamsen H, et al. (2012) Peptidyl-prolyl isomerase Pin1 controls down-regulation of conventional protein kinase C isozymes. *J Biol Chem* 287:13262–13278.
31. Gould CM, Kannan N, Taylor SS, Newton AC (2009) The chaperones Hsp90 and Cdc37 mediate the maturation and stabilization of protein kinase C through a conserved PXXP motif in the C-terminal tail. *J Biol Chem* 284:4921–4935.
32. Banky P, et al. (2003) Related protein-protein interaction modules present drastically different surface topographies despite a conserved helical platform. *J Mol Biol* 330: 1117–1129.
33. Newlon MG, et al. (2001) A novel mechanism of PKA anchoring revealed by solution structures of anchoring complexes. *EMBO J* 20:1651–1662.
34. Sarma GN, et al. (2010) Structure of D-AKAP2:PKA RI complex: Insights into AKAP specificity and selectivity. *Structure* 18:155–166.
35. Boeshans KM, Resing KA, Hunt JB, Ahn NG, Shabb JB (1999) Structural characterization of the membrane-associated regulatory subunit of type I cAMP-dependent protein kinase by mass spectrometry: Identification of Ser81 as the in vivo phosphorylation site of RIalpha. *Protein Sci* 8:1515–1522.
36. Taylor SS, Kornev AP (2011) Protein kinases: Evolution of dynamic regulatory proteins. *Trends Biochem Sci* 36:65–77.
37. Knighton DR, et al. (1991) Structure of a peptide inhibitor bound to the catalytic subunit of cyclic adenosine monophosphate-dependent protein kinase. *Science* 253: 414–420.
38. Michel JJ, Scott JD (2002) AKAP mediated signal transduction. *Annu Rev Pharmacol Toxicol* 42:235–257.
39. Huang LJ, Durick K, Weiner JA, Chun J, Taylor SS (1997) D-AKAP2, a novel protein kinase A anchoring protein with a putative RGS domain. *Proc Natl Acad Sci USA* 94: 11184–11189.
40. Aye TT, et al. (2009) Selectivity in enrichment of cAMP-dependent protein kinase regulatory subunits type I and type II and their interactors using modified cAMP affinity resins. *Mol Cell Proteomics* 8:1016–1028.
41. Miki K, Eddy EM (1999) Single amino acids determine specificity of binding of protein kinase A regulatory subunits by protein kinase A anchoring proteins. *J Biol Chem* 274: 29057–29062.